Conference Proceedings

Solar World Congress 2015
Daegu, Korea, 08 – 12 November 2015

Performance Analysis of Concave Cavity Surface Receiver for a Non – imaging Solar Concentrator

K. S. Reddy and T. Srihari Vikram

Heat Transfer and Thermal Power Laboratory, Department of Mechanical Engineering,

Indian Institute of Technology Madras, Chennai – 600 036, INDIA

Abstract

In the present study, a numerical investigation of concave surface cavity receiver of non-imaging solar concentrator is carried out considering various operating and geometrical parameters such as mass flow rate of the fluid, solar radiation and receiver configuration. The fluid outlet temperature, pressure drop across the coil for different receiver configurations are studied along with the heat loss estimation of concave cavity surface receiver for non-imaging concentrating collector. The convective and radiative heat loss from the receiver surface is calculated based on 3-D numerical simulations. For helical receiver, the temperature rise is found to be 30°C (0.5kg/min) and 17°C (1kg/min) respectively; whereas for helical-spiral receiver, the temperature rise is found to be 27°C (0.5 kg/min) and 15°C (1 kg/min). The pressure drop across the coil ranges between 1kPa to 14kPa for different mass flow rate and solar radiation for two configurations of the receiver. The present model can be used for estimating the heat transfer and fluid flow characteristics of helical receiver for EHC.

Keywords: Solar energy, Non-imaging collectors, concave cavity surface receiver, Process heat

1. Introduction

The use of conventional fuels such as oil for process heat applications is slowly finding their way to the renewable energy means. One of the most promising renewable energy sources is solar thermal which can be widely used for variety of applications ranging from process heating to power generation. IRENA (2015) briefs that solar thermal can fulfill the process heat demands irrespective of its geographic location. It discusses the technical highlights, process and technology status detailing about the various options for process heat applications. It also presents a brief insight of various process heat systems installed all around the world. Lauterbach et al., (2010) reports that industrial sector is one of the most promising application for solar process heat application. Solar thermal heat is used for the following broad categories of industrial applications such as “heating of fluid streams”, “heating of baths/vessels” and “drying” and studied the feasibility of solar collectors for the industrial applications (Lauterbach et al., 2011). The development of new collectors provides scope for its use in industrial process heat applications. The emergence of new medium temperature collectors provides opportunities for the use of solar thermal energy because they can supply higher temperature demands and can co-exist with the installed high temperature heat networks (Martinez et al, 2012).

Non-imaging optics involves the design of optical components for solar concentrating systems. For given concentration ratio, non-imaging optics provides wide acceptance angles for solar applications. A non-tracking, non-imaging solar concentrator with low heat loss has been proposed and its optical and thermal performance has been investigated by Ustaoglu et al., (2015). It was found that the absorber temperature is uniform and with a concentration ratio of 2.51, the concentrator, even at an absorber temperature of 373 K, operates with an average efficiency of 47.8%, although the absorber is assumed to have a gray surface. The concentrator’s thermal efficiency has been compared with that of other solar collectors, and found to be higher than that of conventional solar collectors. Kaiyan et al., (2011) presented a novel multiple curved

doi:10.18086/swc.2015.10.11 Available at http://proceedings.ises.org

surfaces compound concentrator. It consists of a parabolic and a flat contour. It consists of focus at the backside which is extremely useful and convenient for some applications. The comparison with traditional paraboloid and CPC has been carried out. Garcia-Botella et al., (2006) presented an analysis of elliptical concentrators studying on concentration ratio and analysed for some applications such as concentrators and illuminators. A new 3-D asymmetric concentrator (hyperbolic concentrator) is studied based on different theories. Based on ray tracing analysis, it has been shown that 3-D concentrator in the shape of hyperbola intercepts maximum incident rays can be used for non-tracking solar application (Garcia-Botella et al., 2009).

Ali et al. (2010) compared the optical performance of 2-D and 3-D elliptical hyperbolic concentrator (EHC) and found that the optical efficiency of 2D and 3D system are 63% and 78% respectively. Ali et al., (2011) presented optical performance of 3D static circular and elliptical hyperboloids. Four different configurations of hyperboloids are studied based on the ray tracing techniques and flux distribution at the receiver aperture has been presented. The parametric studies have been carried out and the optical efficiency of the systems have been compared and have been compared and evaluated. It has been found that elliptical hyperboloid performs better than other three configurations. A detailed parametric study on the elliptical hyperbolic concentrator has been performed by Ali et al., (2013). The overall performance of the concentrator was assessed based on the acceptance angle, effective concentration ratio and optical efficiency. Optimization of the concentrator profile and geometry has also carried out to improve the overall performance and flux distribution at receiver aperture for different geometric parameters have also been presented. The optical efficiency of the system has been estimated to be 27% with concentration ratio of 20x and wide range of incidence angles (±30°).

Helical coil receiver was proposed for solar desalination applications using elliptical hyperboloid concentrators (Reddy et al., 2014). 2-D ray tracing has been carried out to study the optical performance of the proposed system and a parametric study has been carried out for fluid flow and heat transfer in helical coil and the system has been optimized for higher performance. The experimental performance investigation of EHC for process heat applications has been carried out by Ali et al., (2014). The maximum stagnation temperature and outlet fluid temperature was found to be 150°C and 90°C at flow rate of 0.5 kg/min. Ray tracing analysis has been carried out to estimate the flux at receiver plane and compared with that of the IR images. Experiments have been carried out for two different flow rates and the outlet temperature of the fluid has been determined.

In the present study, a numerical investigation of concave cavity surface receiver with helical and spiral coils used in elliptical hyperbolic concentrator (EHC) is carried out considering various operating and geometrical parameters such as mass flow rate, solar radiation, receiver configuration etc. and the outlet temperature of the fluid and the pressure drop across the receiver coil has been estimated. The heat loss analysis from the concave cavity surface receiver has also been carried out to study the performance of the concave cavity surface receiver by varying the incident solar radiation and emissivity of the surface.

2. Modelling of Helical – Spiral coil for Elliptical Hyperbolic Concentrator

2.1 Elliptical Hyperbolic Concentrator

Elliptical Hyperbolic Concentrator (EHC) consists of a hyperbolic concentrator with elliptical aperture both at top and bottom and a receiver placed at the bottom to collect the incident solar energy and convert to useful thermal energy. The receiver consists of helical coil which is wound in a elliptical shape to capture the incident concentrated solar radiation. The schematic of side view of the elliptical hyperbolic concentrator system is shown in Fig.1. The working fluid flows through the bottom of the receiver and gets heated due to

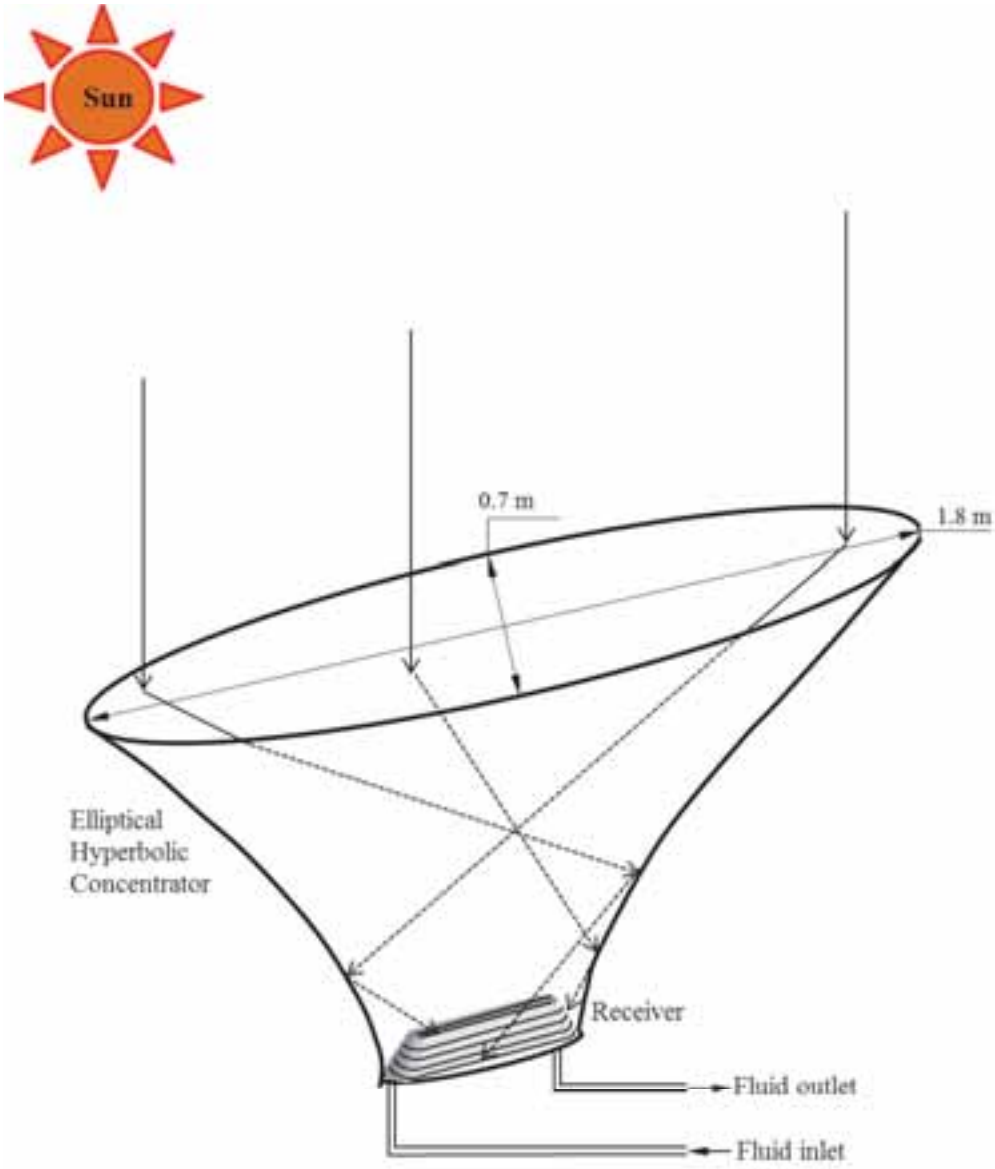

Fig. 1: Elliptical Hyperbolic Concentrator system (side view)

the incident solar energy and leaves at the top. EHC is a non-imaging concentrating collector having wide acceptance angle and does not require tracking.

2.2 Modelling of Helical-Spiral Coil

The helical receiver is a concave cavity surface receiver consisting of copper tube (Diameter: 6mm, No. of helical turns: 7; spiral turns: 5) wound in the elliptical shape (Fig. 2) is placed in the bottom aperture of EHC. The receiver coil is wound over a trapezoidal metal plate to hold in proper position. The trapezoidal metal plate forms a concave cavity. The working fluid (water) enters the receiver coil at the bottom and leaves at the top. The front view and bottom view of the concave cavity surface is shown in Fig. 2 and the helical coil receiver with and without spiral coil is shown in Fig. 3

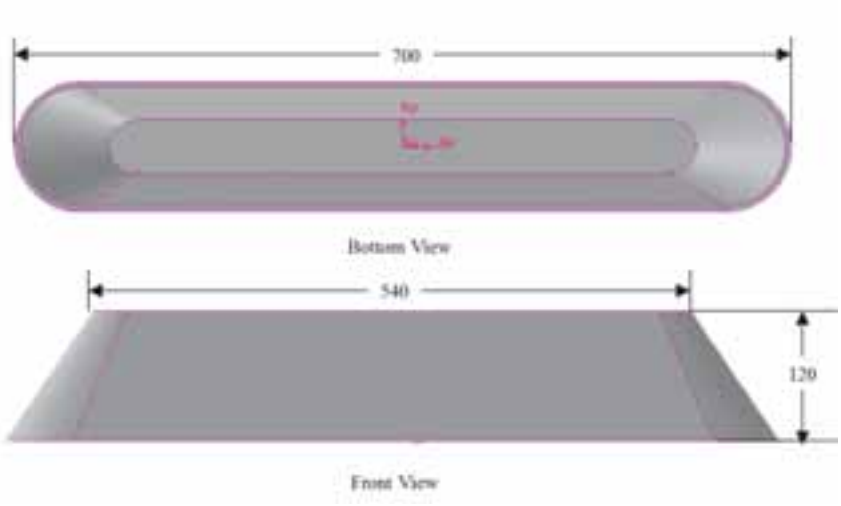

Fig. 2: Concave cavity surface receiver

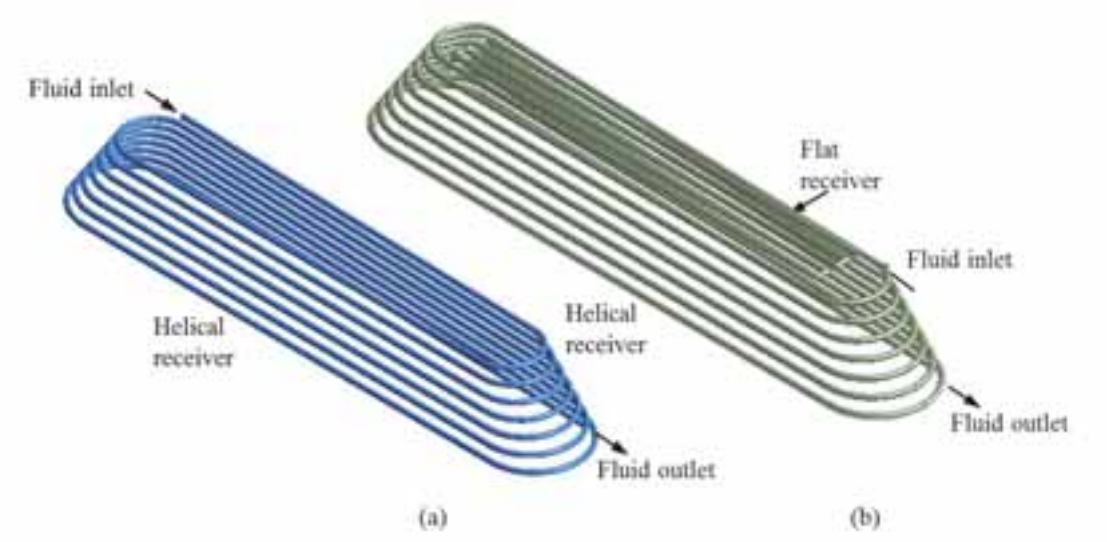

Fig. 3: Helical coil receiver (a) without spiral (b) with spiral

The geometry of the concave cavity surface receiver has been modelled using modelling software, GAMBIT 2.4.6. The helical coil receiver has been modelled using ANSYS Workbench V14.5.

2.3 Mathematical model

The flow and heat transfer simulations are carried out by solving the system of governing equations simultaneously:

Continuity equation is given by:

$$\nabla \cdot \vec{V} = 0 \qquad \text{(eq.1)}$$

Momentum equation is given by:

$$\vec{V} \cdot \nabla(\rho \vec{V}) = -\nabla p + \mu . \nabla^2 \vec{V} + \rho \vec{g} + \vec{F}_c \qquad \text{(eq.2)}$$

Energy equation is given by:

$$\vec{V} \cdot \nabla(\rho C_p T) = k \nabla^2 T \qquad \text{(eq. 3)}$$

The laminar, steady state and 3-D governing equations are solved in ANSYS FLUENT V14.5 using an implicit solver. Along with the above-mentioned conditions, surface-to-surface radiation model is also incorporated to account for the radiation exchange between the surfaces of the concave cavity surface receiver.

2.4 Boundary Conditions

The concentrated solar radiation falls on the concave cavity surface receiver placed at the bottom aperture of EHC. Hence the outer surface of the trapezoidal cavity is subjected to heat flux and the bottom surface of the cavity surface is insulated to minimize the heat loss from the receiver. To account for the effect of atmosphere, a spherical domain is considered which is 5 m in radius. This model has been used to estimate the heat losses from the receiver. Similarly to account for fluid flow and heat transfer analysis, the receiver coil is subjected to various boundary conditions. As the receiver coil is wound around the trapezoidal (concave cavity) surface, the concentrated solar flux is applied on the outer walls of the receiver coil. The mass flow rate is specified at the inlet of the receiver at the bottom and the pressure outlet is set at the outlet of the receiver at the top. The computational domain and boundary conditions of the concave cavity surface receiver and receiver coil are shown in Fig. 4.

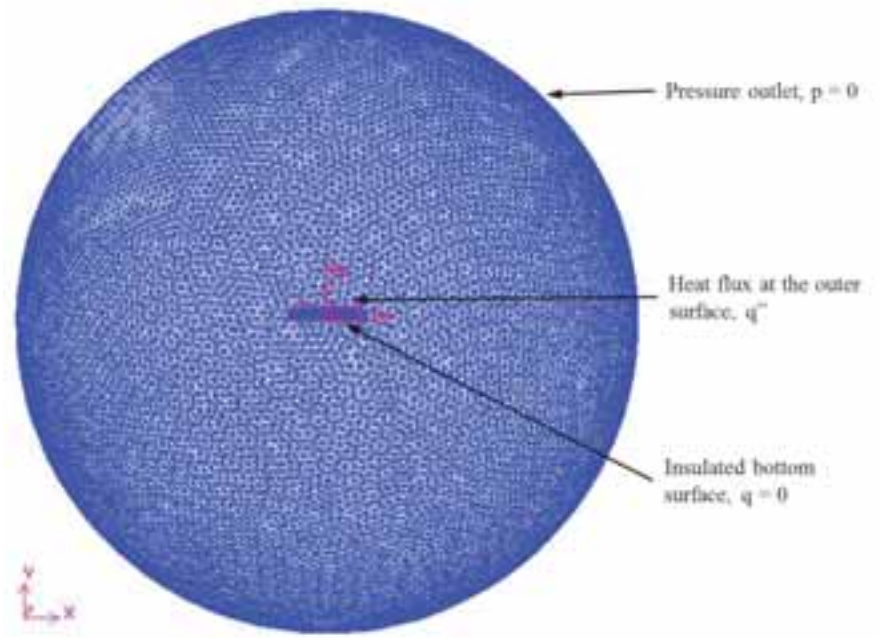

(a)

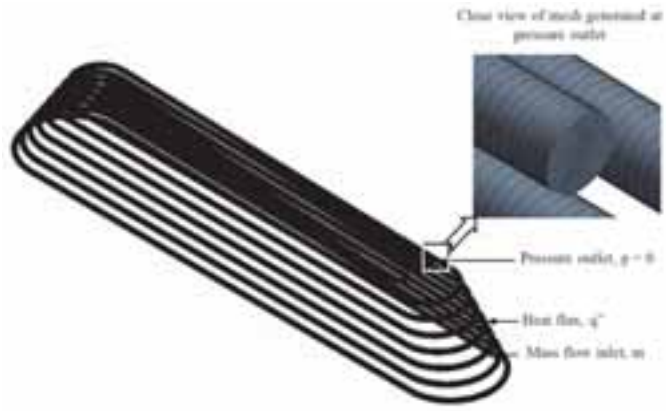

(b)

Fig. 4 : Computational domain and boundary conditions (a) Concave cavity surface receiver (b) Helical – Spiral receiver coil

2.5 Numerical Procedure

The computational domain of the concave cavity surface is created using GAMBIT 2.4.6. The atmosphere surrounding the concave cavity surface receiver is modelled such that the cavity receiver is placed inside large spherical domain. The size of the external domain is increased until it had an insignificant effect on the working fluid and heat flows from the receiver. In the present analysis, external domain is considered as 5 m diameter based on the numerical simulations. The fine mesh is considered for the receiver and coarse mesh is considered for outer atmosphere/domain. The computational domain of concave cavity surface considered in the present study is shown in Fig. 4. For pressure velocity coupling, SIMPLE algorithm has been used, with body force weighted algorithm for discretization of pressure with first order upwinding scheme for the discretization of equations. For the fluid flow simulations, A convergence criterion of 10^{-3} was imposed on the residuals of the continuity equation, momentum equation. A convergence criterion of 10^{-6} is considered for energy equation. The present numerical procedure for heat loss from concave cavity surface receiver is validated with Reddy and Kumar model (2009) and found to vary within acceptable limits. The present numerical procedure is validated with two different models (i) conical tube bundle and (ii) spiral coil. The fluid flow and heat transfer characteristics of conical tube bundle has been studied by Ke et al, 2011. The heat transfer and heat transfer coefficient obtained by Ke et al (2011) for the inlet flow velocity of 0.1 m/s has been compared with the present numerical procedure and the results are tabulated (Table 1) and shows good agreement. The heat transfer and flow characteristics of spiral coil carried out by Naphon (2011) is compared at flow rate of 0.05 kg/s. Table 1 shows the comparison of experimental and numerical results for heat transfer rate and outlet temperature of the spiral coil.

Tab. 1: Validation of numerical procedure

Parameter	Ke et al, 2011	Present numerical procedure	Naphon, 2011	Present numerical procedure
Heat transfer coefficient (W/m^2K)	150	152.46	-	-
Heat transfer (W)	307.45	310.35	2785.25	3031.72
Outlet fluid temperature (°C)	-	-	34.65	35

3. Performance analysis of concave cavity surface receiver

3.1 Heat loss analysisfrom concave cavity surface receiver

The 3-D numerical simulations have been carried out to estimate the heat losses from the concave cavity surface receiver. The effect of the parameters like DNI and emissivity of the receiver are varied to study the heat losses from the concave cavity receiver.

The heat losses from the receiver are estimated based on the following equations:

$$Q_{total} = h_{total} A_s (T_w - T_a) \quad \text{(eq.4)}$$

$$Q_{rad} = h_{rad} A_s (T_w - T_a) \quad \text{(eq.5)}$$

$$Q_{conv} = Q_{total} - Q_{rad} \quad \text{(eq.6)}$$

3.1.1 Effect of solar radiation

The effect of solar radiation on the heat loss from the concave cavity receiver is studied by varying the incident solar flux on the surface of the concave cavity surface receiver. Fig. 5 shows the temperature contours of the concave cavity surface receiver for solar radiation of $250 W/m^2$ at theoretical maximum heat flux of 10150 W/m^2. The maximum surface temperature at the receiver is about 470 K. Fig. 6 shows the temperature contours of the concave cavity surface receiver for solar radiation of 1000 W/m^2 at maximum heat flux of $40607 W/m^2$ incident on the receiver. The maximum surface temperature on the receiver is about 933K.

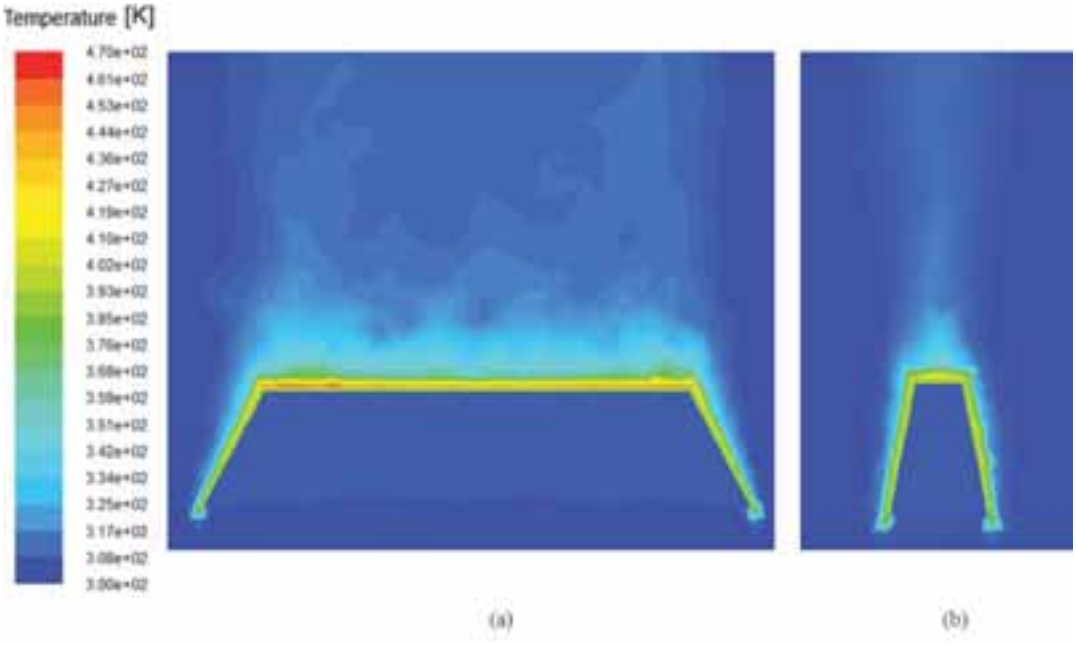

Fig. 5: Temperature contours of concave cavity surface receiver at different planes for DNI = 250W/m^2 (a) Z = 0 (b) X = 0

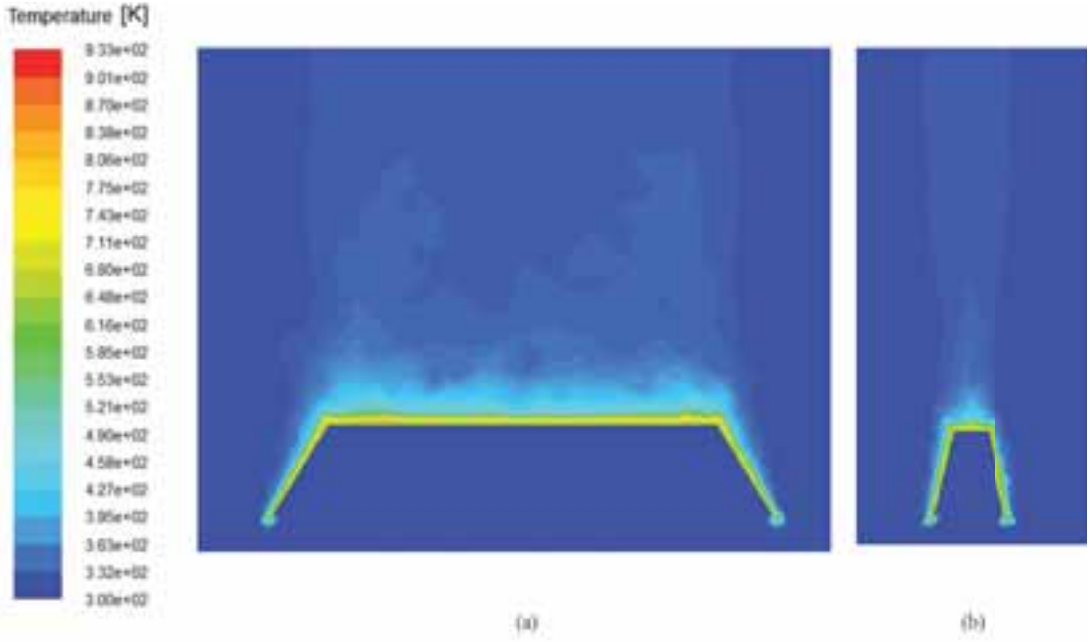

Fig. 6: Temperature contours of concave cavity surface receiver at different planes for DNI = 1000W/m^2 (a) Z = 0 (b) X = 0

3.1.2 Effect of emissivity of receiver surface

The emissivity of the receiver surface is varied to study the effect on heat loss from the receiver surface. The emissivity of the receiver surface is set to 1 as it is coated with black matt paint. The temperature contours for receiver at an emissivity of 1 for average heat flux value is shown in Fig. 7

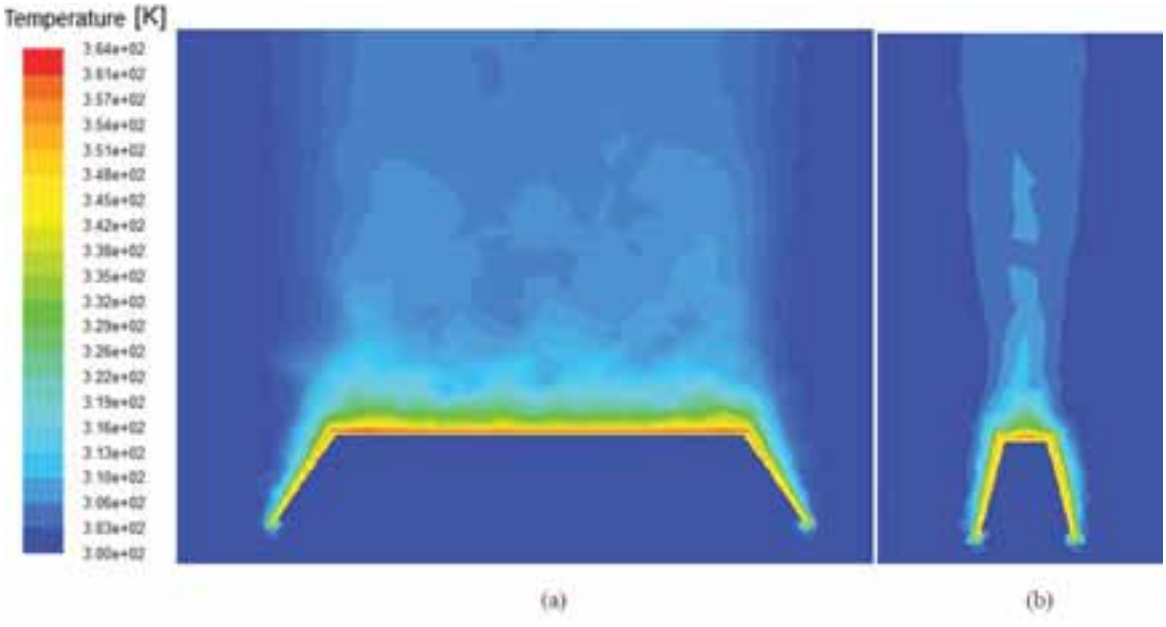

Fig. 7: Temperature contours of receiver (ε =1) at different planes for DNI = 1000W/m^2 (a) Z = 0 (b) X = 0

The comparison of heat losses and the maximum temperature in the receiver surface is calculated and tabulated in Table 2. The values correspond to the average heat flux incident on the receiver surface.

Tab. 2: Comparison of parameters for different DNI and emissivity

Parameter	DNI = 250 W/m^2		DNI = 1000 W/m^2	
	ε = 0	ε = 1	ε = 0	ε = 1
Maximum Temperature (°C)	70	44	123	112
Convective Heat loss (W)	28	28	111	111
Radiative Heat loss (W)	-	17	-	65
Surface temperature of receiver (°C)	47	44	113	91

3.2 Fluid flow and heat transfer analysis of helical-spiral coil receiver

The fluid flow and heat transfer analysis have been carried out to estimate the outlet temperature of the fluid and the pressure drop across the coil. The two types of coil configuration are studied to study the performance of the system.

3.2.1 Effect of solar radiation

The incident solar radiation on the receiver surface is varied to study the effect on the receiver performance. The solar radiation values of 250 W/m^2 and 1000 W/m^2 are considered in the present study. The outlet temperatures are calculated for two different configurations are estimated. For helical receiver, the temperature rise of 57°C (0.5kg/min) and 38°C (1kg/min) is observed for 1000W/m^2. At solar radiation of 500 W/m^2, the temperature rise is found to be 30°C (0.5kg/min) and 17°C (1kg/min) respectively. The effect of solar radiation incident on the receiver is studied and found that there is temperature difference of 27°C for twice increase in solar radiation.

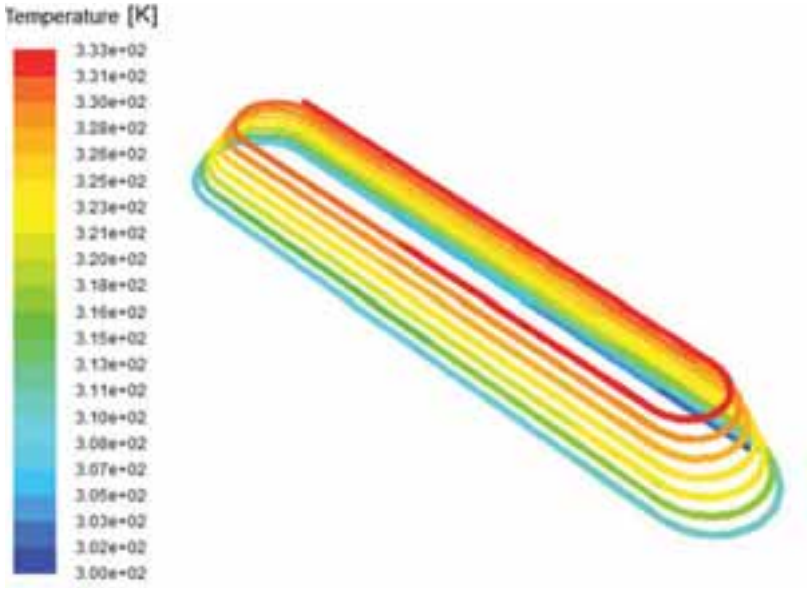

Fig. 8: Temperature contours of helical receiver for DNI of 500W/m^2

3.2.2 Effect of flow rate

The effect of flow rate on the receiver performance has been carried out. The flow rate values of 0.5 and 1 kg/min have been considered for the present analysis. Based on the flow rate, it is observed that at solar radiation of 250W/m^2, the temperature rise was found to be about 27°C and a pressure drop of 13023 Pa for 0.5 kg/min and temperature rise of 17°C and pressure drop of 14062 Pa was observed for 1 kg/min. For twice the mass flow rate, the variation of average fluid temperature is about 20°C for helical receiver.

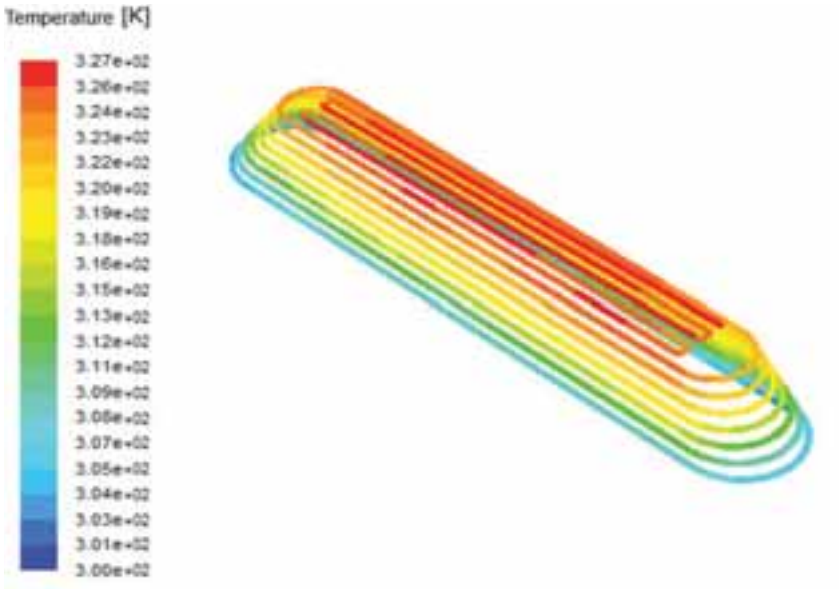

(a)

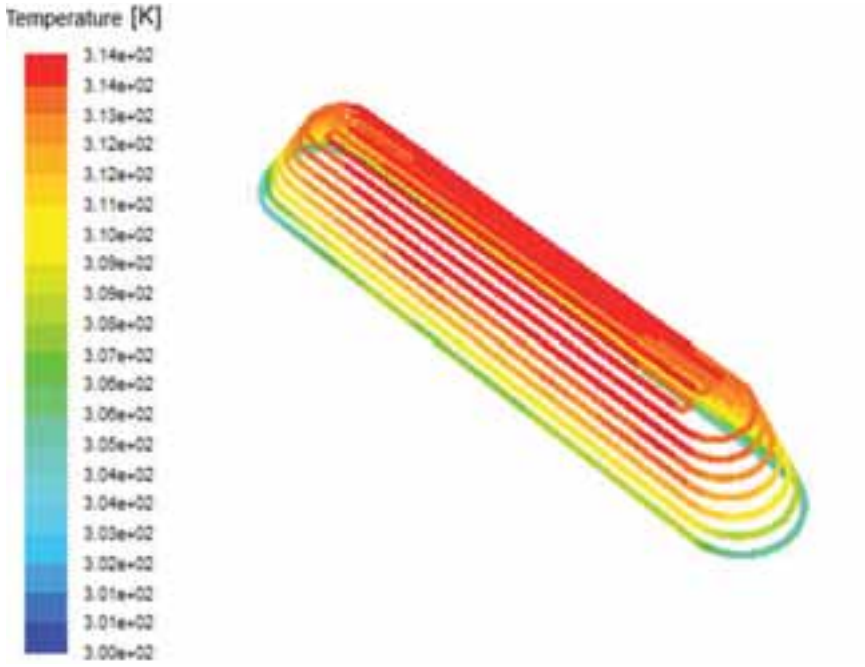

(b)

Fig. 8: Temperature contours of helical - spiral receiver surface for different flow rates and DNI = 250W/m^2

(a) 0.5 kg/min (b) 1 kg/min

The variation of the temperature of the fluid along the coil length for the helical receiver is shown in Fig. 7. It is observed that, for the flow rate of 0.5 kg/min, the outlet fluid temperature is 87°C and for 1 kg/min, it is about 65°C.

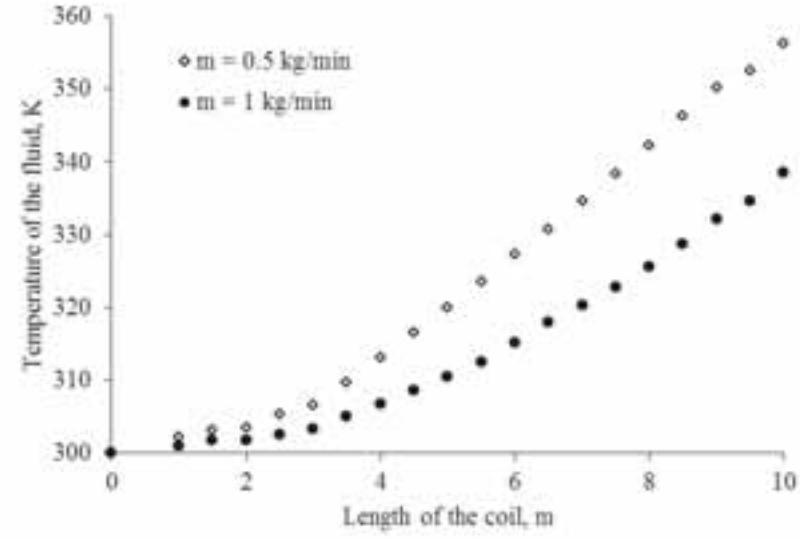

Fig. 9: Variation of average fluid temperature along coil for helical receiver

3.3 Performance investigation of helical-spiral coil receiver

The performance investigation of the helical-spiral receiver is carried out considering the useful heat transfer to the fluid and the heat loss from receiver comprising of the conductive, convective and radiative heat losses from the system. The heat collection efficiency of the receiver is given by (Reddy at al., 2014):

$$\text{Heat collection efficiency} = \frac{\text{Energy absorbed by the fluid}}{\text{Energy incident on the receiver}} \qquad \text{(eq. 7)}$$

Based on the analysis, it is found that receiver heat collection efficiency is about 84%.

4. Conclusion

In the present study, 3-D numerical investigations have been performed to study the heat loss from the concave cavity receiver surface and the fluid outlet temperature and the pressure drop across the helical coil. The heat loss analysis from the concave cavity surface receiver has been carried out by varying the incident solar radiation and emissivity of the surface. The study has been carried out for different parameters such as different solar insolation values, emissivity of the receiver surface and flow rates. Based on the analysis, For helical receiver, the temperature rise is found to be 30°C (0.5kg/min) and 17°C (1kg/min) respectively; whereas for helical-spiral receiver, the temperature rise is found to be 27°C (0.5 kg/min) and 15°C (1 kg/min). The pressure drop for helical receiver varies between 1kPa to 8kPa and 3kPa to 14 kPa for helical-spiral receiver. The present 3-D model can be used to study the performance of the helical coil receiver for elliptical hyperbolic concentrator.

Nomenclature:

C_p	Specific heat capacity (J/kgK)
$\vec{F}_c$	Centrifugal force (N)
g	Acceleration due to gravity (m/s^2)
k	Thermal conductivity (W/mK)
m	Mass flow rate (kg/min)
p	Pressure (Pa)
q''	Heat flux (W/m^2)
Q	Heat losses from the receiver (W)
T	Temperature (°C or K)
$\vec{V}$	Velocity vectors

Greek symbols

ε	Emissivity
ρ	Density (kg/m^3)

Subscripts

a	ambient
conv	convective
rad	radiative
total	total

5. References

Ali, I.M.S., Kew, P.A., O'Donovan, T.S., Reddy, K.S., Malick, T.K., 2010. Optical performance evaluation of a 2-D and 3-D novel hyperboloid solar concentrator, In: World Renewable Energy Congress XI, Abu Dhabi, 1738–1743

Ali, I.M.S., O'Donovan, T.S., Reddy, K.S., Mallick, T.K., 2010, Optical performance of circular and elliptical 3-D static solar concentrators. National Solar Conference, American Solar Energy Society, Arizona, USA.

Ali, I.M.S., O'Donovan, T.S., Reddy, K.S., Mallick, T.K., 2013. An optical analysis of a static 3D concentrator, Solar Energy, 88, 57–70.

Ali, I.M.S., Vikram, T.S., O'Donovan, T.S., Reddy, K.S., Mallick, T.K., 2014. Design and experimental analysis of a static 3-D elliptical hyperboloid concentrator for process heat applications, Solar Energy, 102, 257–266.

Eames, P. C., Norton, B., 1993. Detailed parametric analyses of heat transfer in CPC solar energy collectors, Solar Energy, 50 (4), 321-338

Garcia-Botella, A., Balbuena, F., Alvarez, A., Vazquez, D., Bernabeu, E., 2009. Ideal 3D asymmetric concentrator, Solar Energy, 83, 113–117.

Garcia-Botella, A., Fernandez-Balbuena, A., A., Bernabeu, E., 2006. Elliptical concentrators, Applied Optics, 45 (29), 7622–7627

IEA-ETSAP and IRENA Technology Brief E21, 2015. Solar Heat for Industrial Processes – A Technology Brief.

Kaiyan, H., Hongfei, Z., Tao, T., 2011. A novel multiple curved surfaces compound concentrator, Solar Energy, 85, 523–529

Lauterbach, C., Schmitt, B., Jordan, U., Vajen, K., 2010. Potential for Solar Process Heat in Germany - Suitable Industrial Sectors and Processes. Proc. EuroSun. Graz.

Lauterbach, C., Javid R., S., Schmitt, B., and Vajen, K., 2011. Feasibility Assessment of Solar Process Heat Applications, Solar World Congress, Kassel.

Martínez, V., Pujol, R., Moià, M., 2012. Assessment of medium temperature collectors for process heat, Energy Procedia, 30, 745 – 754.

Reddy, K.S., Mallick, T.K., Vikram, T.S., Sharon, H., Design and optimisation of elliptical hyperboloid concnetrator with helical receiver, Solar Energy, 108, 515-524

Ustaoglu, A., Okajima, J., Zhang, X.-R., Maruyama, S. 2015. Performance evaluation of a nonimaging solar concentrator in terms of optical and thermal characteristics. Environ. Prog. Sustainable Energy. doi: 10.1002/ep.12236